

II. THE ELECTRON-PROTON INELASTIC SCATTERING EXPERIMENT

A. Introduction

Group A desires to conduct a survey of inelastic electron-scattering from the proton. The method of investigation will consist of measuring the spectra of inelastically scattered electrons as a function of the four-momentum transfer and energy transfer to the target system. Such studies have been previously carried out at the Mark III accelerator and at the CEA. In the Stanford work⁽¹⁾ the (3,3) resonance was excited and studied as a function of four-momentum transfer up to about 0.79 (BeV/c). The CEA experiment⁽²⁾ observed, in addition, evidence for the excitation of the 1.512- and 1.688-BeV resonances at four-momentum transfers up to about 1.97 (BeV/c); however, the measurements at the higher momentum transfers are limited by poor statistics. Because the inelastic cross section contains q^2 dependences which are similar to that of the form factors describing elastic scattering, the counting rates drop rapidly as a function of four-momentum transfer. The higher energies and intensities available at SLAC will enable both the scope and the precision of the measurements of e-p inelastic scattering to be greatly enlarged.

B. Theoretical Considerations and Counting Rates

Using the representation given by Hand⁽¹⁾ the cross section for inelastic scattering can be expressed (within the approximation of one-photon exchange) as

$$\frac{d^2\sigma}{d\Omega dE'} = \Gamma_t(q^2, k) \sigma_t(q^2, k) + \Gamma_s(q^2, k) \sigma_s(q^2, k)$$

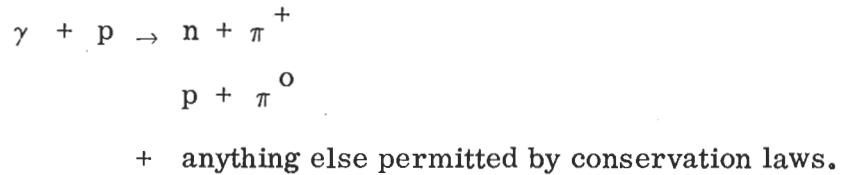
where

$$\Gamma_t \equiv \frac{\alpha}{4\pi^2} \frac{k}{q^2} \frac{E'}{E} \left[2 + \frac{\text{ctn}^2 \frac{\theta}{2}}{1 + \frac{(E - E')^2}{q^2}} \right]$$

and

$$\Gamma_s \equiv \frac{\alpha}{4\pi^2} \frac{k}{q^2} \frac{E'}{E} \left[\frac{\text{ctn}^2 \frac{\theta}{2}}{1 + \frac{(E - E')^2}{q^2}} \right]$$

Γ_t and Γ_s are the virtual photon spectra associated with the transverse and scalar parts respectively of the electron's interaction. The Γ 's have the dimensions of number of virtual photons/BeV-sr. The quantities σ_t and σ_s can be regarded as cross sections for transitions induced by transverse and scalar virtual photons. The kinematic quantities used in the formula are expressed in the laboratory. They are E , the incoming electron energy; E' , the energy of the scattered electron; θ , the electron scattering angle; q^2 , the square of the four-momentum transfer where $q^2 = 2EE' (1 - \cos \theta)$; k , the laboratory photon energy which produces the same excitation in the center of mass system in the limit of $q^2 \rightarrow 0$, $\sigma_t(k, 0)$ is interpreted to be the total photoproduction cross section, i. e., the cross section for



The FNW⁽³⁾ theory calculates the electro-production of the (3,3) resonance by means of dispersion relations. At present there is no comparable theoretical treatment of electroproduction for higher energy excitations. As a result some of the more recent measurements⁽²⁾ have been analyzed with the use of the following semi-empirical expression (in analogy with the electro-excitation of nuclear levels)

$$\sigma_t(q^2, k) = \left(\frac{q^*}{q^*(0)} \right)^\ell G_{MV}^2(q^2) \sigma_\gamma(k)$$

where G_{MV} is the elastic isovector magnetic form factor of the nucleon, and q^* is the three-momentum transfer in the rest frame of the isobar and $q^*(0)$ is the value of q^* in the limit $q^2 \rightarrow 0$. The CEA group finds that $\ell = 2$ gives reasonable agreement with their observations of the first three resonances as a function of four-momentum transfer. As a guide to estimating cross sections and counting rates, we have used this formula. Experimentally determined total photoproduction cross sections were used in the calculations. Typical counting rates expected with the use of the 20-BeV/c spectrometers are shown for the first two resonances, at 1.238 BeV and 1.512 BeV respectively,

in the attached graphs, Figs. 1-4. Because of the factor $[q^*/q^*(0)]^2$ these rates are probably optimistic at large q^2 . To provide a conservative estimate of the counting rates, a second calculation was made with $[q^*/q^*(0)]^2$ replaced by 1. The predictions of this model are also shown in Figs. 1-4.

A new theoretical approach for interpreting inelastic electron scattering measurements has been given by Bjorken and Walecka.⁽⁴⁾ They have calculated the differential cross section (assuming one-photon exchange) for the process $e + p \rightarrow e + p_R$ where p_R is a nucleon resonance characterized by parity, spin J , and mass M_R . The result is an analogue of the description of e^- - p elastic scattering by the Rosenbluth formula and is given by

$$\left(\frac{d\sigma}{d\Omega}\right)_{\text{LAB}} = \frac{\alpha^2 \cos^2 \frac{\theta}{2}}{4E^2 \sin^4 \frac{\theta}{2}} \left(\frac{E'}{E}\right) \left\{ \frac{q^4}{q^{*4}} |f_c|^2 + \left(\frac{q^2}{2q^{*2}} + \frac{M_R^2}{M^2} \tan^2 \frac{\theta}{2} \right) \left[|f_+|^2 + |f_-|^2 \right] \right\}$$

This formula applies when only the final electron is detected. The form factors $|f_c|$ and $|f_{\pm}|$ of the $\gamma - N^* - p$ vertex are the analogues of G_E and G_M for elastic scattering and are only functions of q^2 . For $q^2 = 0$ the transverse form factors $|f_{\pm}|$ are related to the photoabsorption cross section integrated over the resonance. This treatment thus has the very useful feature of explicitly separating the dependences on energy transfer and four momentum transfer. Detailed properties of the form factors $|f_c|$ and $|f_{\pm}|$ are highly model dependent. However, in the limit $q^* \rightarrow 0$ the form factors have simple threshold behaviors (as a function of q^*) depending on the parity and J of the resonance. Thus low q^2 measurements can possibly shed light on the J and parity of a given resonance to the extent that the limit $q^2 \rightarrow 0$ adequately corresponds to the non-physical limit $q^* \rightarrow 0$. Measurements at higher q^2 will provide information about the dynamics of the process. The q^2 dependence of these form factors will provide a basis for the future theoretical development.

C. Objectives of Measurements

The initial objectives of the electron-proton inelastic scattering program are

1. Search For New Nucleon Resonances.

It is conceivable that in inelastic electron scattering certain resonances may be more easily excited at higher q^2 . Thus, resonances which have not been

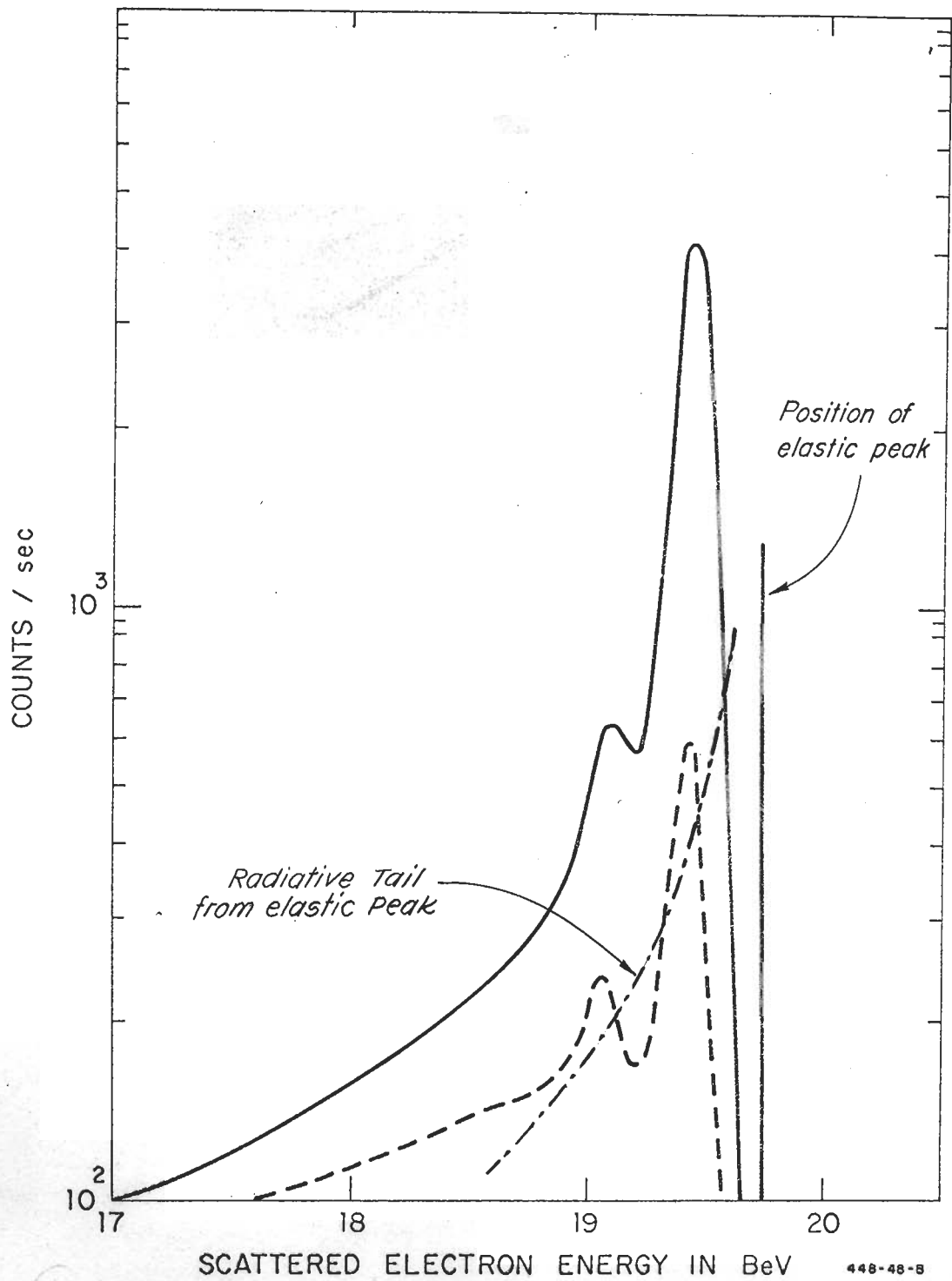


Fig. 1--Number of inelastically scattered electrons expected per sec with the 20-BeV/c spectrometer at incident energy $E_0 = 20$ BeV, $\theta = 2^\circ$, 20 cm long liquid hydrogen target, and 2×10^{13} primary electrons/sec. The spectrum shown in dashed line is obtained by setting $q^*/q^*(0) = 1$. In both spectra, the radiative corrections are not included. The radiative tail from the elastic peak is separately shown.

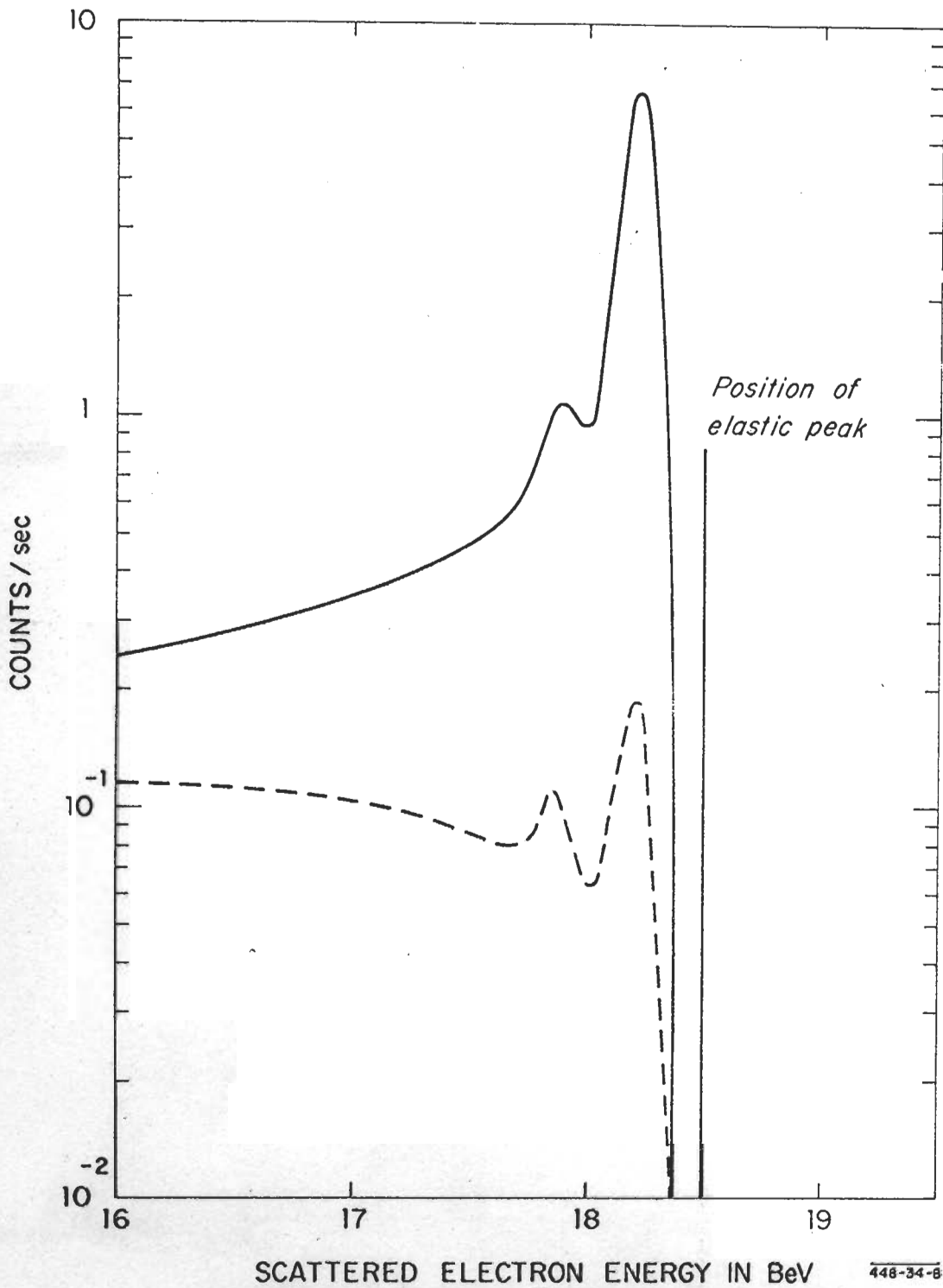


Figure 2--Number of inelastically scattered electrons expected per sec with the 20 BeV/c spectrometer at incident energy $E_0 = 20$ BeV, $\theta = 5^\circ$, 20 cm long liquid hydrogen target, and 2×10^{13} primary electrons/sec. The spectrum shown in dashed line is obtained by setting $q^*/q^*(0) = 1$. In both spectra, the radiative corrections are not included.

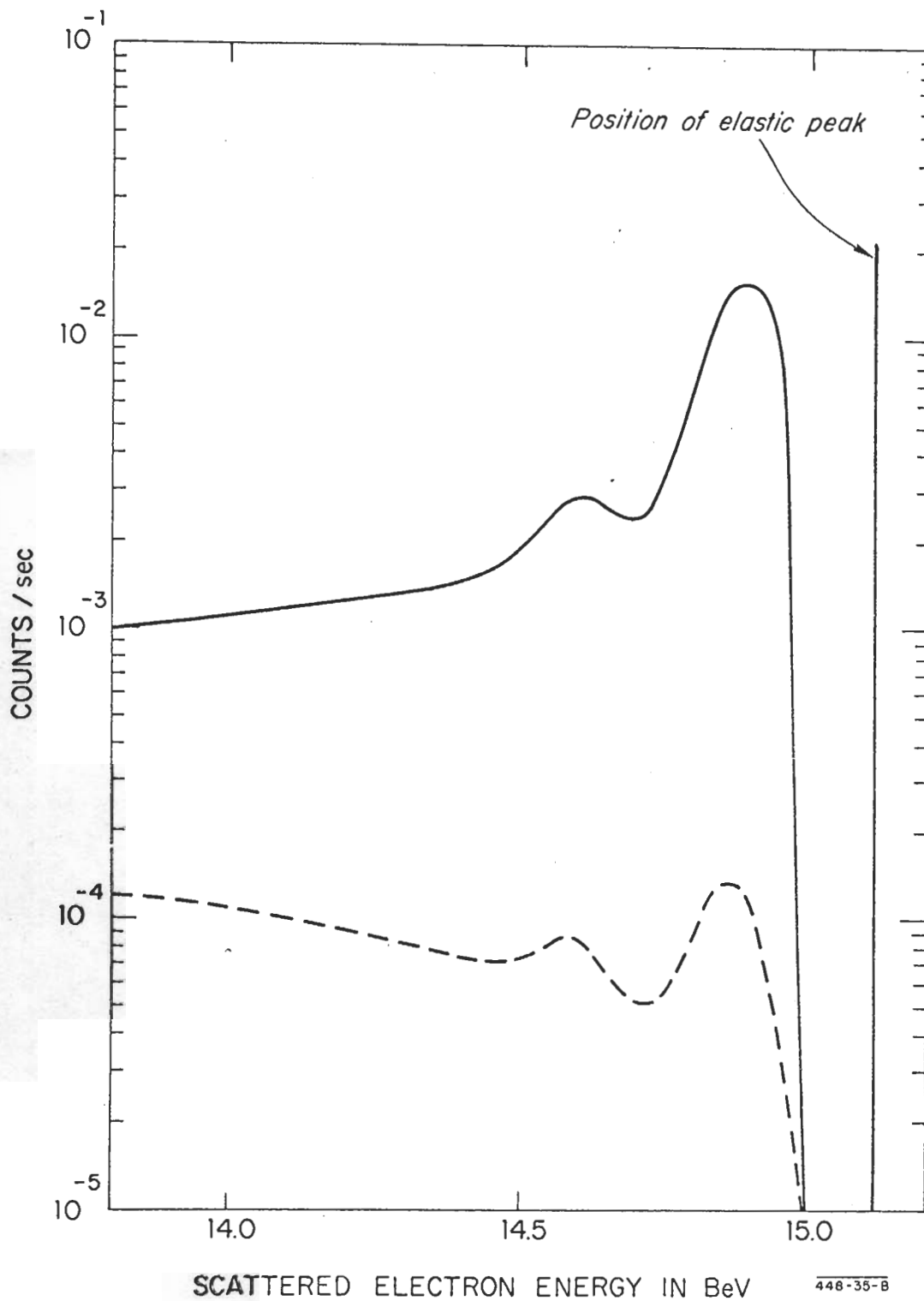


Figure 3--Number of inelastically scattered electrons expected per sec with the 20 BeV/c spectrometer at incident energy $E_0 = 20$ BeV, $\theta = 10^\circ$, 20 cm long liquid hydrogen target, and 2×10^{13} primary electrons/sec. The spectrum shown in dashed line is obtained by setting $q^*/q^*(0) = 1$. In both spectra, the radiative corrections are not included.

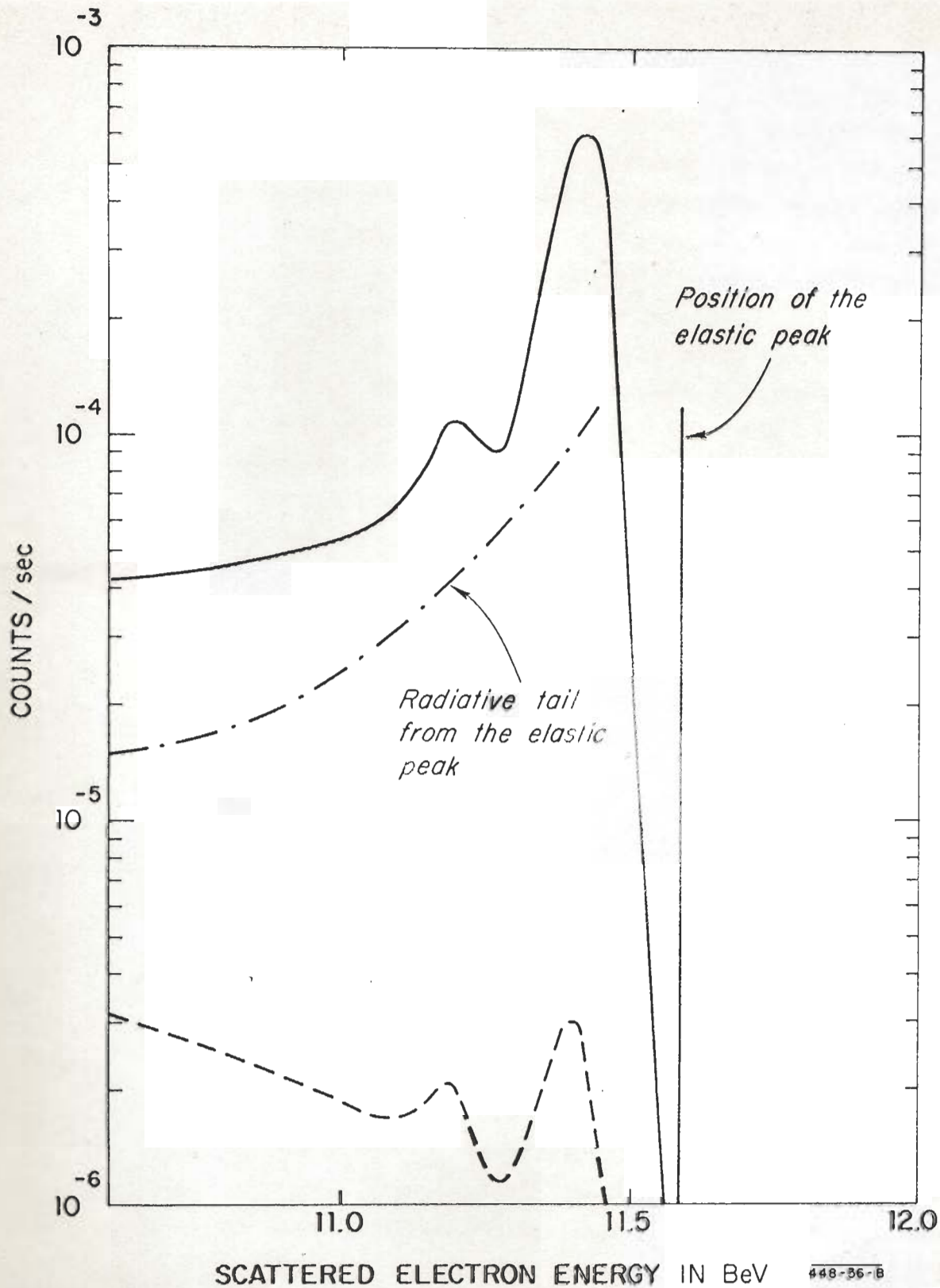


Figure 4--Number of inelastically scattered electrons expected per sec with the 20 BeV/c spectrometer at incident energy $E_0 = 20$ BeV, $\theta = 15^\circ$, 20 cm long liquid hydrogen target, and 2×10^{13} primary electrons/sec. The spectrum shown in dashed line is obtained by setting $q^*/q^*(\theta) = 1$. In both spectra, the radiative corrections are not included. The radiative tail from the elastic peak is separately shown.

seen in photoproduction experiments may be observed in the electroproduction process. An example of selective excitation of resonances as a function of four-momentum transfer has been observed in p-p scattering at CERN by Bellettini⁽⁵⁾, et al. At four momentum transfers of ≤ 1 BeV/c they did not observe the 1.238- and 1.512-BeV resonances; instead, a new resonance of mass ~ 1.400 BeV was observed. However, at momentum transfers ≥ 2 BeV/c the 1.238-, 1.512- and 1.688-BeV resonances are all clearly seen with no evidence of the 1.400-BeV state. In our e-p inelastic scattering program we intend to search for resonances over as wide range of masses and q^2 as is permitted by the kinematics and the backgrounds, with the greatest concentration of effort in the mass region above 1.800 BeV. This would be done by measuring the scattered electron spectra at a variety of specified angles. Because of the narrow widths of the inelastic peaks (as compared to the scattered energy) such a measurement of a given inelastic peak occurs at an approximately constant q^2 over the width of the peak. Since the counting rate at a given q^2 and a given excitation of the nucleon is proportional to the square of the incident energy, it is useful to use the highest energy and the smallest angle that provide the desired q^2 . The relative importance of the background yields will probably be less at the smaller angles, which provides another reason to select high incident energies and small scattering angles. We thus will use the 20-BeV/c spectrometer and make measurements in the angular range of 2° to 15° with an incident energy of 20 BeV. This range of measurements spans a range of four-momentum transfer squared from about 0.4 to about $16 (\text{BeV}/c)^2$. When it becomes of interest to extend the measurements to angles beyond 15° , it will be advantageous to use the 8-BeV/c spectrometer because of its larger solid angle of acceptance.

Table I gives the known nucleon resonances; the percentage separations of the corresponding inelastic electron scattering peaks from the elastic peak, $(E_{\text{el}} - E_{\text{R}})/E_{\text{el}}$, where E_{el} is the elastic scattering energy, and E_{R} is the energy of the inelastic peak; and the effective percentage widths, $\Delta E_{\text{R}}/E_{\text{R}}$, of the corresponding inelastic scattering peaks. ΔE_{R} corresponds roughly to the full width at half maximum of the inelastic peak. The values given in Table I are for an incident energy of 20 BeV.

TABLE I

Mass of Nucleon Isobars in BeV	Isospin and Angular Momentum (T, J)	$\frac{E_{el} - E_R}{E_{el}}$ (%)	$\frac{\Delta E_R}{E_R}$ (%)
1.238	(3/2, 3/2)	1.73	0.80
1.512	(1/2, 3/2)	3.75	1.0
1.688	(1/2, 5/2)	5.25	0.95
1.920	(3/2, 7/2)	7.47	1.9
2.190	(1/2, 7/2)	10.5	2.6
2.360	(3/2, 9/2)	12.5	2.8
2.650	(1/2, 9/2)	16.6	3.4
2.325	(3/2, 11/2)	19.0	4.8

It is clear from the above table that the highest available resolution is not required for these measurements, since the nucleon resonances tend to be relatively wide. A percentage spread as large as 0.3 percent in the incident beam energy would enhance the counting rates without seriously degrading the shape and definition of the inelastic peaks.

2. Measurements of the Inelastic Form Factors as a Function of q^2

As has been discussed, important information can be obtained from the separation and measurement of $|f_c|^2$ and the combination $|f_+|^2 + |f_-|^2$. The quantities $|f_+|^2$ and $|f_-|^2$ cannot be separated in an experiment using unpolarized protons and in which only the final electron is detected. The data obtained in the search for resonances can be used with additional measurements made at larger angles and lower incident energies to separate and evaluate the inelastic form factors as a function of q^2 . If the separation requires measurements at angles larger than 15° we will continue the program with the use of the 8-BeV/c spectrometer. In separating the form factors we will utilize the straight line approach used in the elastic scattering program. We plot at constant q^2

$$\frac{1}{\sigma_{NS}} \left(\frac{d\sigma}{d\Omega} \right) = \frac{q^2}{q^{*2}} \left[\frac{|f_+|^2 + |f_-|^2}{2} + \frac{q^2}{(q^*)^2} |f_c|^2 \right] + \frac{M_R^2}{M^2} \tan^2 \frac{\theta}{2} \left[|f_+|^2 + |f_-|^2 \right]$$

as a function of $\tan^2 \frac{\theta}{2}$. The slope is

$$\frac{M_R^2}{M^2} \left[|f_+|^2 + |f_-|^2 \right]$$

and the intercept is

$$\frac{q^2}{q^{*2}} \left[\frac{|f_+|^2 + |f_-|^2}{2} + \frac{q^2}{q^{*2}} |f_c|^2 \right].$$

This approach will also allow us to test the one-photon exchange approximation which requires a straight line fit. When more information becomes available we will develop optimization computer programs which will allow us to determine the range of θ which will minimize the running time for a given precision in the determination of $|f_c|^2$ and $|f_+|^2 + |f_-|^2$, in complete analogy with what we have done in designing the e^-p elastic scattering experiment.

D. Experimental Plan

We plan to use the 20-BeV/c spectrometer in the first phase of this experiment. The target will be a 20-cm-long liquid hydrogen target. We plan to measure the cross section in the angular range of 2 to 15° and at incident energies from 10 to 20 BeV in the initial phase. The percentage energy spread will be set at 0.1% at low q^2 points where the counting rates are high and at about 0.3% at the higher four-momentum transfer measurements. First we will search for resonances up to the highest possible masses at various values of q^2 . We will then make the additional measurements required for the determination of the inelastic form factors as a function of q^2 . Measurements will be attempted in the range of q^2 from 0.4 to 16 (BeV/c)².

The electron-proton inelastic scattering program covers a large range of kinematic variables. It will probably require a large amount of effort and machine time to make a complete and systematic study. Since no adequate models exist for predicting the inelastic scattering counting rates, it is not possible to estimate at this time the amount of machine time required to complete the initial phase of the program. We would thus like to request 250 hours of running time to make initial survey measurements.

The experiment should give sufficient information for much more detailed future proposals dealing with more specific inelastic scattering experiments.

E. Backgrounds

Unlike elastic scattering, the inelastic scattering process allows no kinematic separation from some of the prominent backgrounds. Thus backgrounds will in general be more troublesome in the inelastic scattering program. The most important backgrounds that are expected are the following:

1. Wide Angle Bremsstrahlung.

This process gives a continuum which consists of the radiative tails from processes occurring at higher scattering energies than that being detected. This background will be more fully discussed in Section F on Radiative Corrections where some numerical examples will be given. To correct the results this background will have to be calculated and subtracted from the data with a radiative correction program.

2. π^- Arising From Multipion Production.

We consider the π^- to arise from peripheral events strongly peaked in the forward direction, and the nonperipheral events roughly isotropic in the center-of-mass system. The peripheral events are ascribed to the Drell process and to the photoproduction of the ρ^0 meson through a diffraction process. The latter process is very strongly peaked at 0° and the angular distribution of the resulting π^- comes from folding the production distribution with the decay distribution. The nonperipheral part is approximated by

$$\frac{\sigma_0}{4\pi} \frac{d\Omega^*}{d\Omega} (\theta, k) = \left(\frac{d\sigma_0}{d\Omega} \right)_{\pi^-}$$

with $d\Omega^*$ and $d\Omega$ representing the differential solid angles in the c.m. and laboratory systems. We take $\sigma_0 = 50 \mu\text{b}$ and assume the π^- has a flat energy distribution, and represent the photoproduction cross section by

$$\frac{d^2\sigma}{d\Omega dE'} = \frac{1}{E_m} \left(\frac{d\sigma_0}{d\Omega} \right)_{\pi^-} \quad \text{where} \quad E_m = \frac{k - \mu}{1 + \frac{k}{m} (1 - \cos \theta)}$$

From this expression we can calculate the counting rates for electroproduction and photoproduction. In Figs. 5-7 are shown curves representing the counting rates resulting from the π^- backgrounds at $\theta = 5^\circ, 10^\circ, 15^\circ$ from peripheral and nonperipheral processes. A beam intensity of 2×10^{13} electrons/sec and a 20-cm-long hydrogen target are assumed. Included in the calculation is a pion detection efficiency of 10^{-4} introduced by our planned $\pi - e$ discriminator.

3. Another Source of Background Results From the Dalitz Decay of the π^0 .

Results from the CEA suggest that single π^0 photoproduction will have a very small cross section at SLAC energies; however there is no way to rule out a sizeable photoproduction cross section for π^0 resulting from multipion photoproduction processes. Unfortunately there are no adequate models to estimate this yield so we will arbitrarily take our values of $(d^2\sigma/d\Omega dE')_{\pi^-}$ to represent the differential cross section for the photoproduction of π^0 . This probably provides a reasonable order of magnitude estimate. To get the yield of Dalitz electrons we insert the factor of 1/80 for the decay probability and assume a flat energy distribution for the resulting electrons. The counting rates for this process are given in Figs. 8-10 for $\theta = 5^\circ, 10^\circ, 15^\circ$ for 2×10^{13} electrons/sec and a 20-cm-long hydrogen target. This background can be eliminated from the data by measuring the positron yields at each point and subtracting these yields from the data.

There exist techniques, due to Panofsky and Allton,⁽¹⁾ to subtract the background experimentally. We can put thin radiators of different thickness in front of the liquid hydrogen target. The extrapolation of the extra counting rate at zero radiator thickness will represent the background. The accuracy of subtraction depends on the running time.

F. Radiative Corrections

The radiative processes result in the following modifications of the inelastic data. The inelastic peak shapes are changed; the symmetrical distributions are given skew shapes with a radiative tail on the low momentum side; however the effective full width at half maximum is not significantly changed. The most important changes are (1) the peak rests on a continuum from the radiative tails of other processes, and (2) the peak height is roughly reduced by the

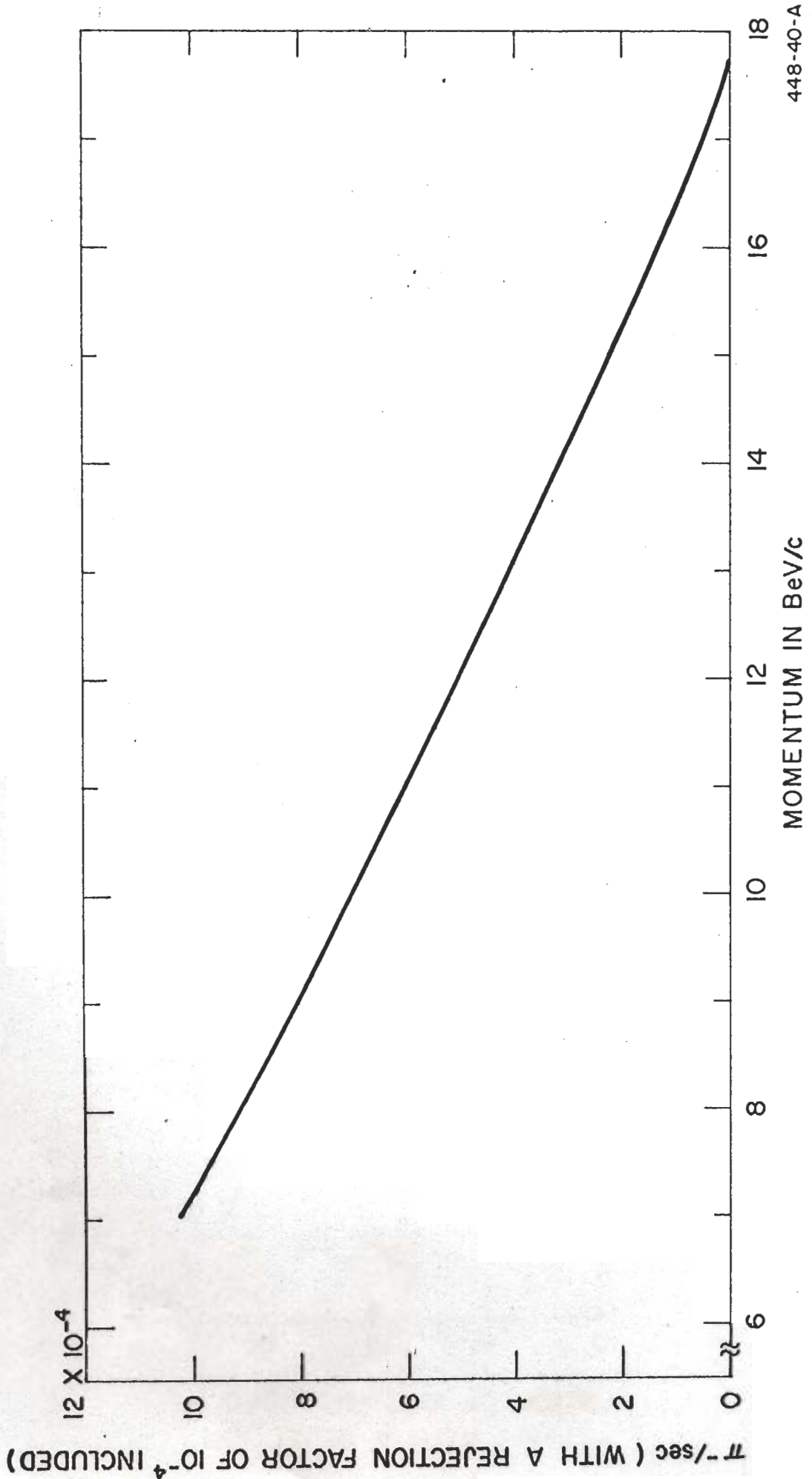


FIG.5 -- NUMBER OF NEGATIVE PIONS DETECTED WITH 0.1% MOMENTUM RESOLUTION, 20 cm LONG LIQUID HYDROGEN TARGET AND 2×10^{13} INCIDENT ELECTRONS / sec AT $\theta = 5^\circ$ AND $E_0 = 20$ BeV

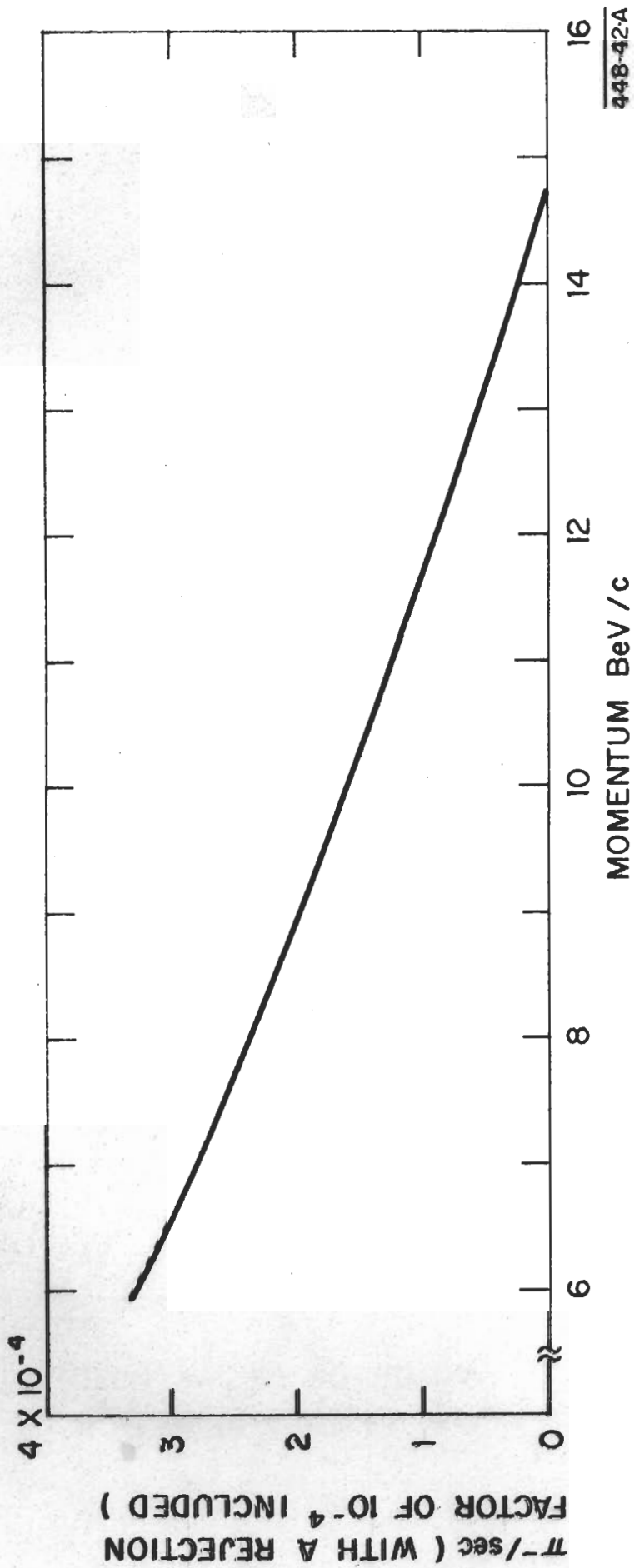


FIG.6-- NUMBER OF NEGATIVE PIONS DETECTED WITH 0.1 % MOMENTUM RESOLUTION,
 20 cm LONG LIQUID HYDROGEN TARGET AND 2×10^{13} INCIDENT ELECTRONS/sec
 AT $\theta = 10^\circ$ AND $E_0 = 20 - \text{BeV}$

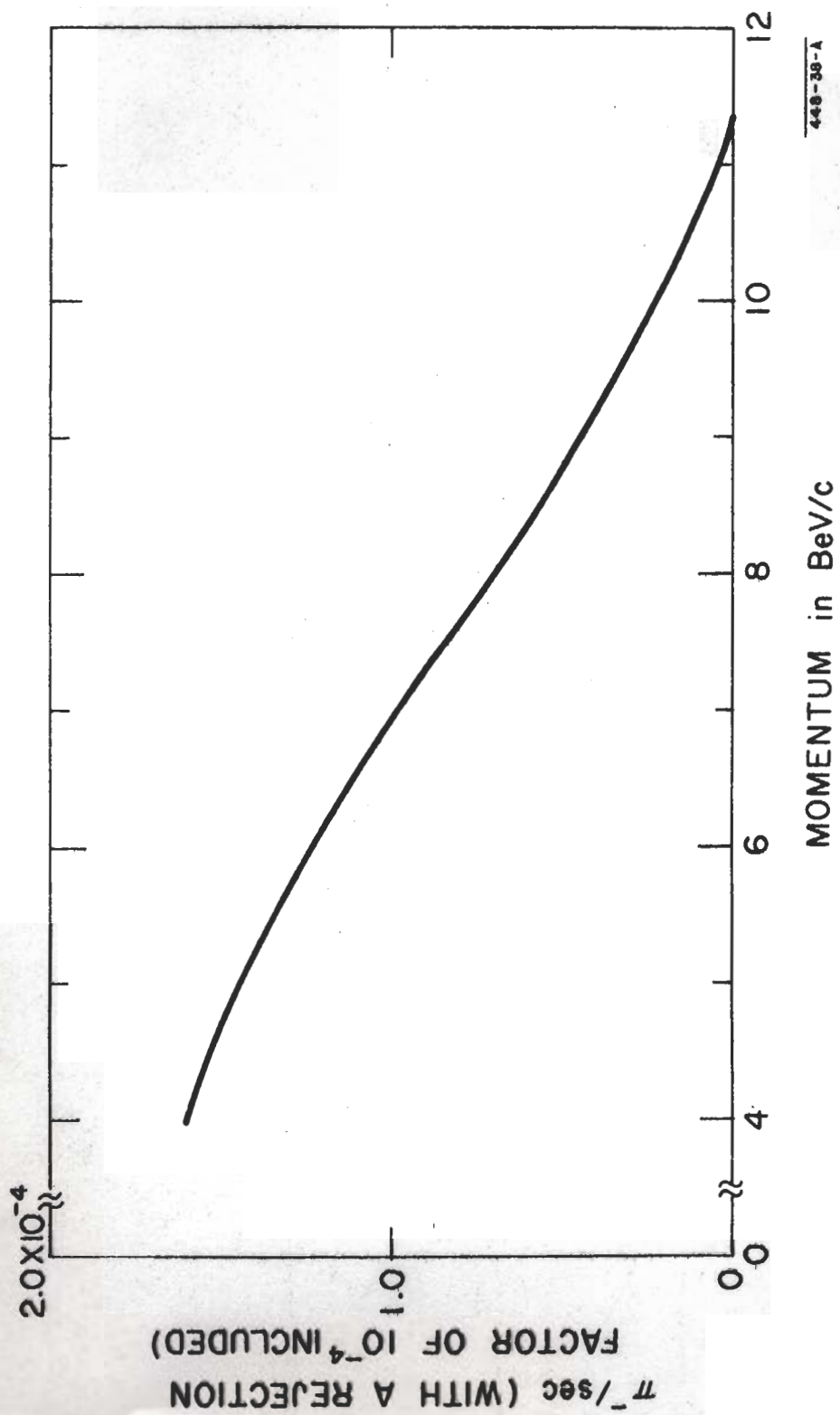


Fig. 7--Number of negative pions detected with 0.1% momentum resolution, 20 cm long liquid hydrogen target, and 2×10^{13} incident electrons/sec at $\theta = 15^\circ$ and $E_0 = 20$ BeV.

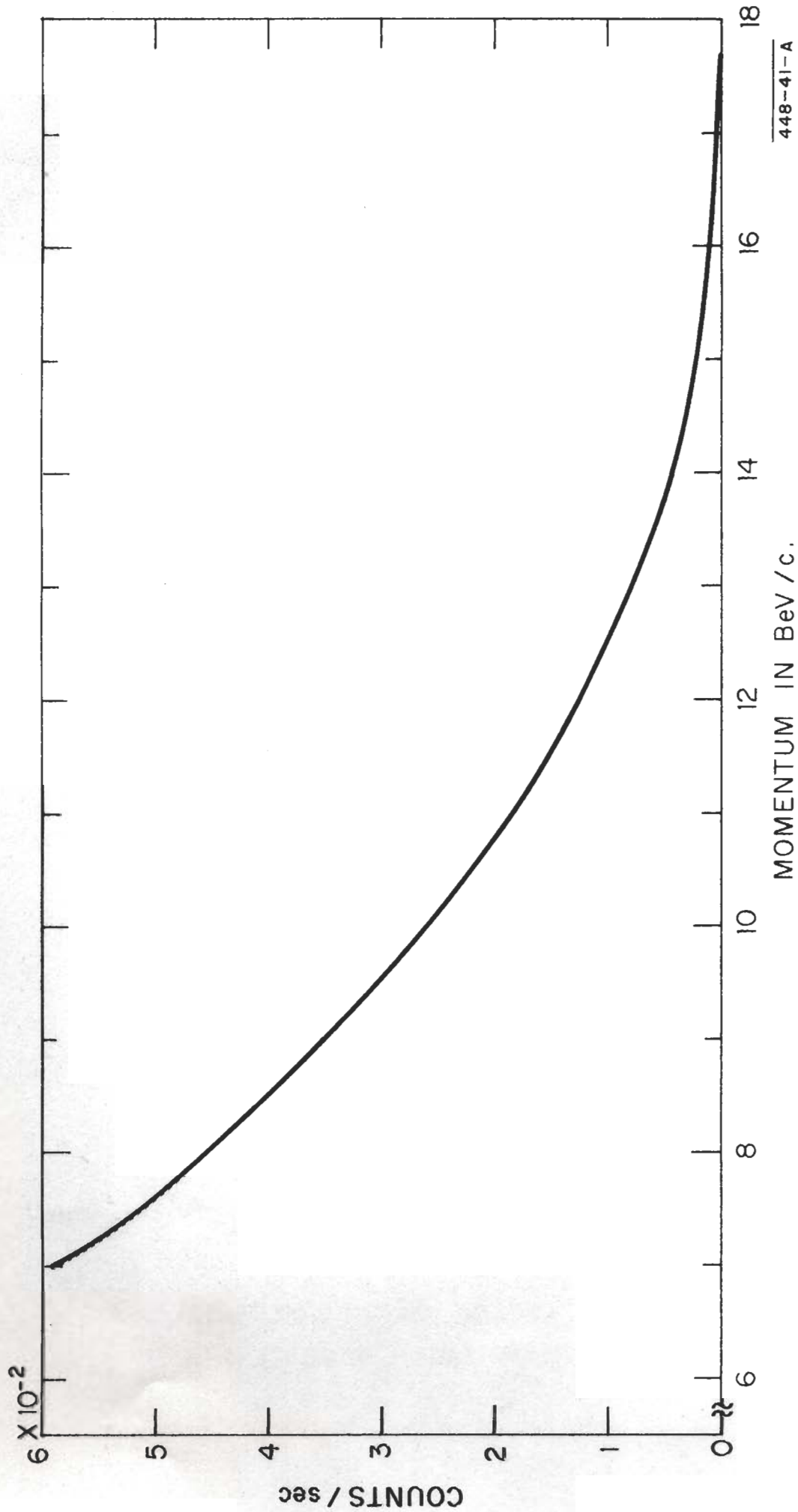
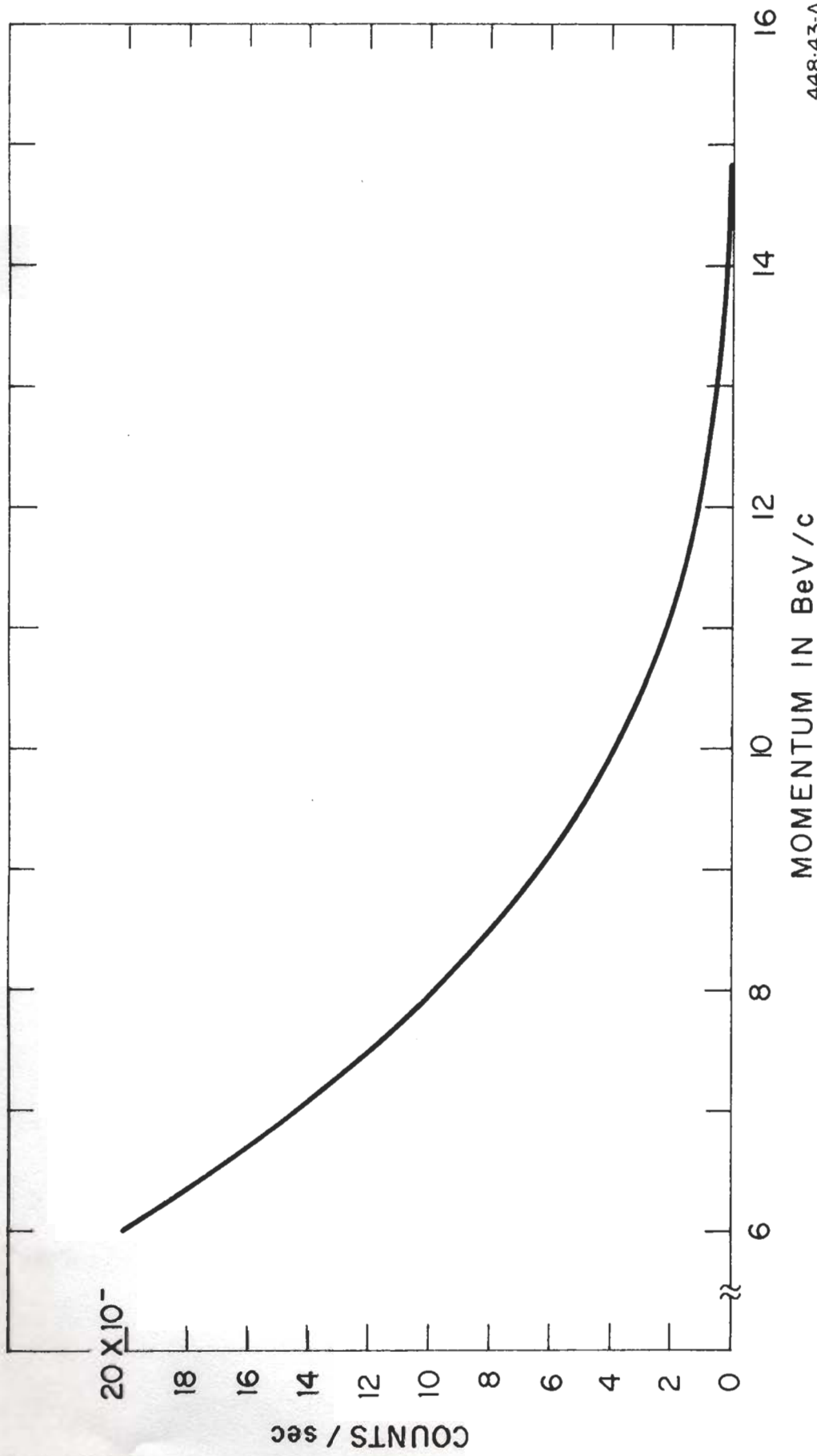
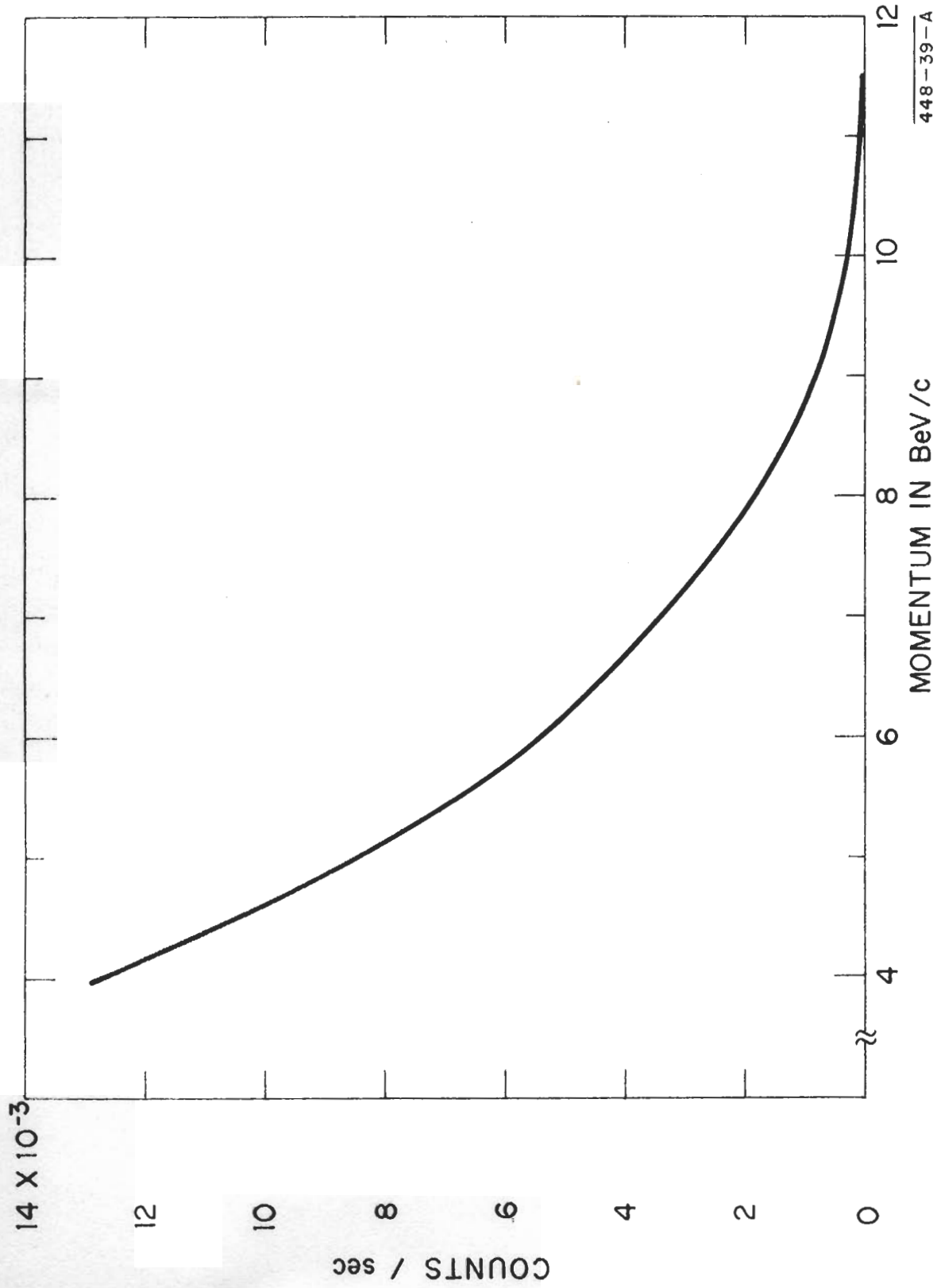


FIG. 8 -- NUMBER OF DALITZ DECAY ELECTRONS DETECTED WITH 0.1% MOMENTUM RESOLUTION,
 20 cm LONG LIQUID HYDROGEN TARGET AN 2×10^{13} INCIDENT ELECTRONS / sec AT $0^\circ = 5^\circ$
 AND $E_0 = 20$ -BeV



448-43-A

FIG. 9 -- NUMBER OF DALITZ ELECTRON DETECTED WITH 0.1 % MOMENTUM REDUCTION,
 20 cm LONG LIQUID HYDROGEN TARGET AND 2×10^{13} INCIDENT ELECTRONS / sec
 AT $\theta = 10^\circ$ AND $E_0 = 20$ - BeV



448-39-A

FIG. 10 -- NUMBER OF DALITZ ELECTRONS DETECTED WITH 0.1%
 MOMENTUM RESOLUTION, 20 cm LONG LIQUID HYDROGEN
 TARGET AND 2×20^{13} INCIDENT ELECTRONS / sec AT $\theta = 15^\circ$
 AND $E_0 = 20$ - BeV

factor of $(1 - \delta_s) e^{-\delta_R}$ where

$$\delta_s = -\frac{2\alpha}{\pi} \left\{ \left(\ln \frac{q^2}{m^2} - 1 \right) \ln \left[\sqrt{n} \frac{\Delta E_R}{E_R} \right] \right\}$$

and

$$\delta_R = -\frac{t}{\ln 2} \ln \sqrt{n} \frac{\Delta E_R}{E_R}$$

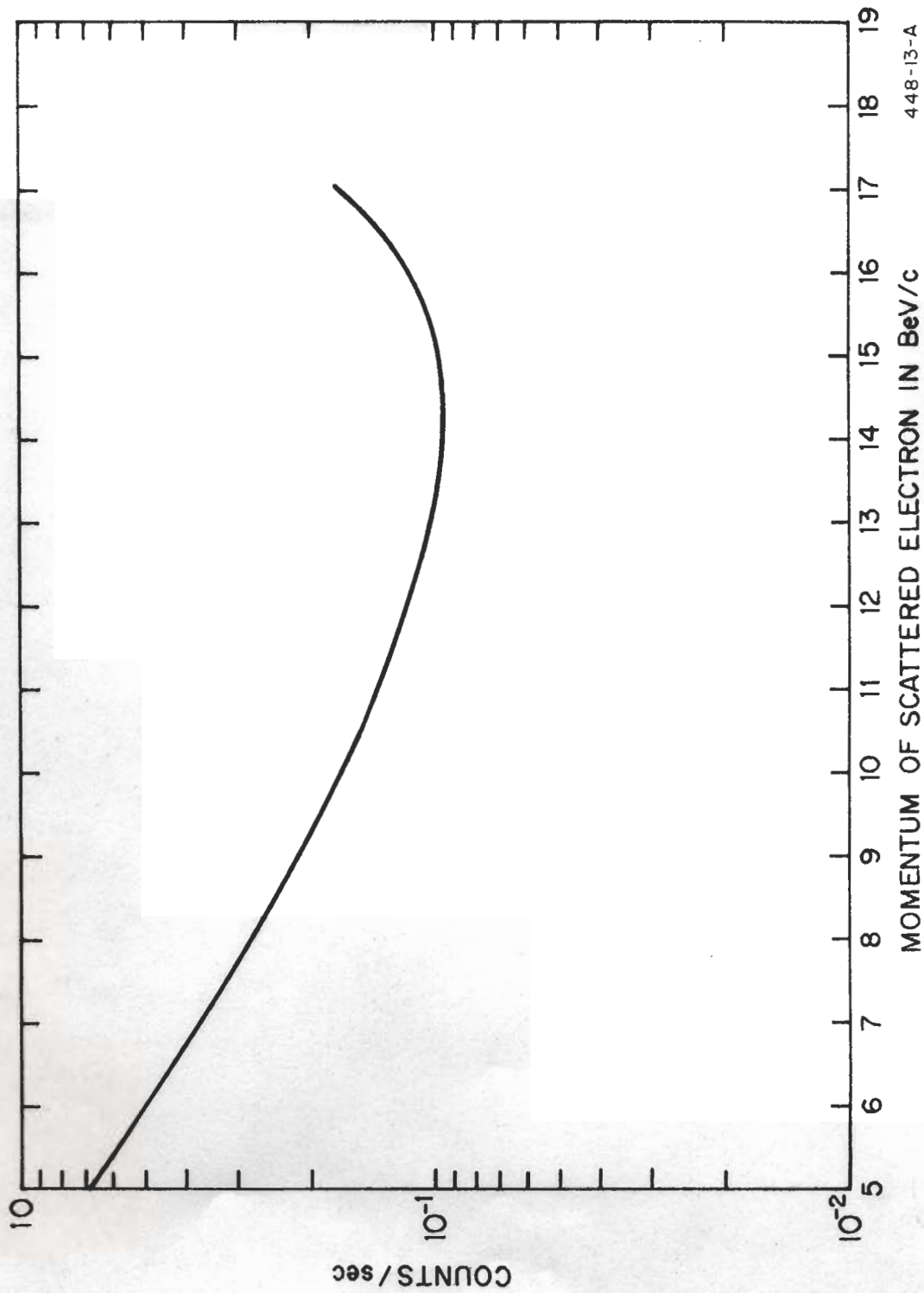
and ΔE_R is roughly the width of the detected inelastic peak; $n = E/E_R$; and t is the number of radiation lengths of the target.

Table II gives the values of δ_s in the range of q^2 considered in this experiment. $\Delta E_R/E_R$ is taken to be .01. A 20-cm-long hydrogen target gives a value of $-\delta_R \approx 14\%$.

TABLE II
INELASTIC ELECTRON SCATTERING

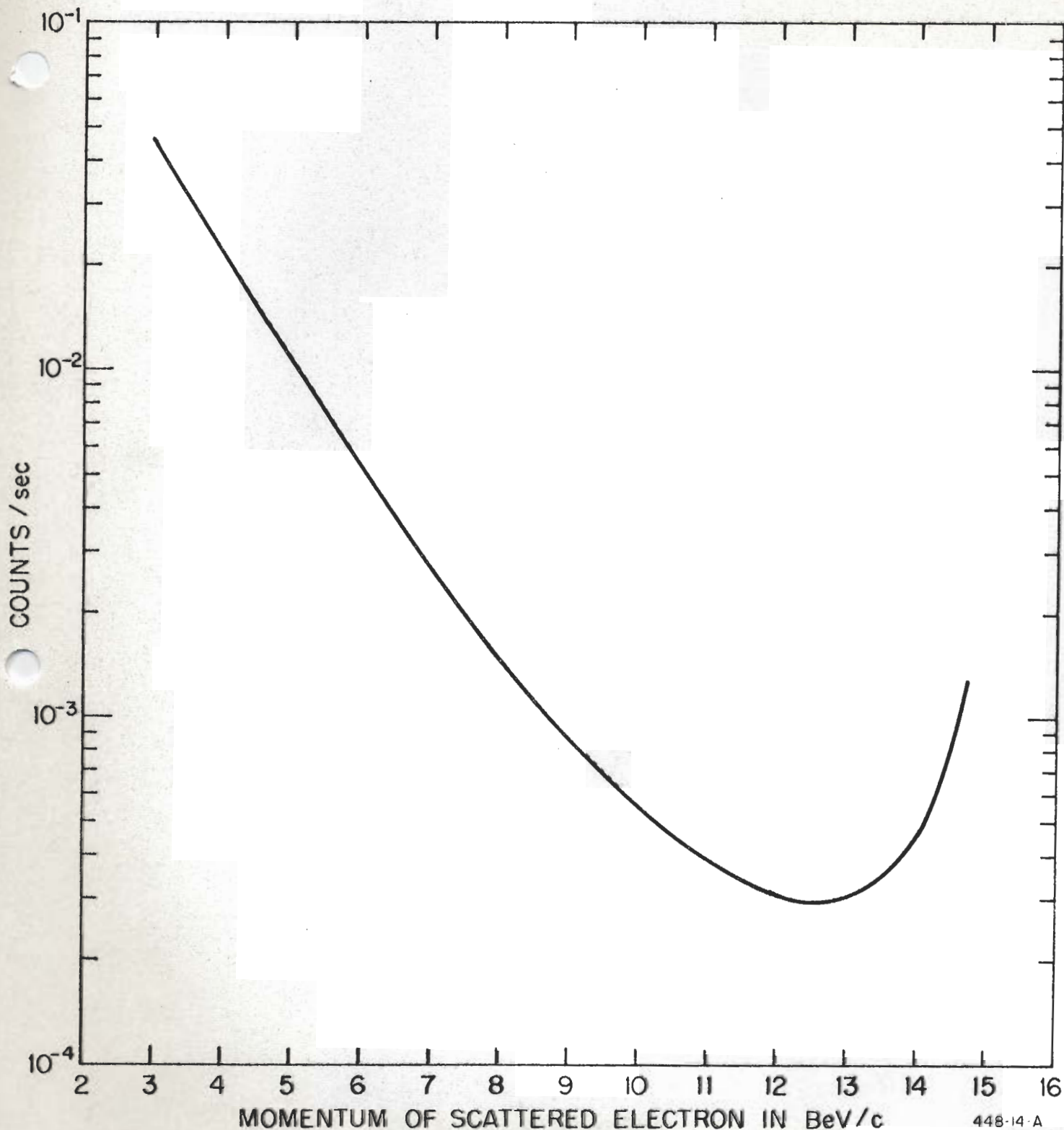
$E_0 = 20 \text{ BeV}$	
q^2 (BeV/c) ²	δ_s
2.81	0.249
9.54	0.260
15.73	0.259
21.05	0.252
24.95	0.244
29.70	0.229
33.10	0.209

The δ_R term makes the major contribution to the radiative effects. Thus we can use a target as long as 40 cm without causing serious problems with respect to the radiative corrections. In Figs. 11-13 the sum of the radiative tails from the elastic peak and the 1.238-BeV inelastic peak are shown for $\theta = 5^\circ, 10^\circ, 15^\circ$. In a further example the total radiative correction to the integrated yield of the 1.238-BeV inelastic peak is shown as a function of q^2 Fig. 14, and in Fig. 15 the peak height (degraded by radiative processing) of the 1.238-BeV inelastic peak is compared to the radiative tail of elastic peak as a function q^2 . A large computer program is being developed at MIT, as part of the Group A collaboration, to make complete radiative corrections to elastic and inelastic scattering data. Appendix V gives a description of this program and some preliminary applications of folding radiative effects into theoretical spectra. Ultimately this program will be able to unfold radiative effects from data or fold radiative effects into theory with high resolution.



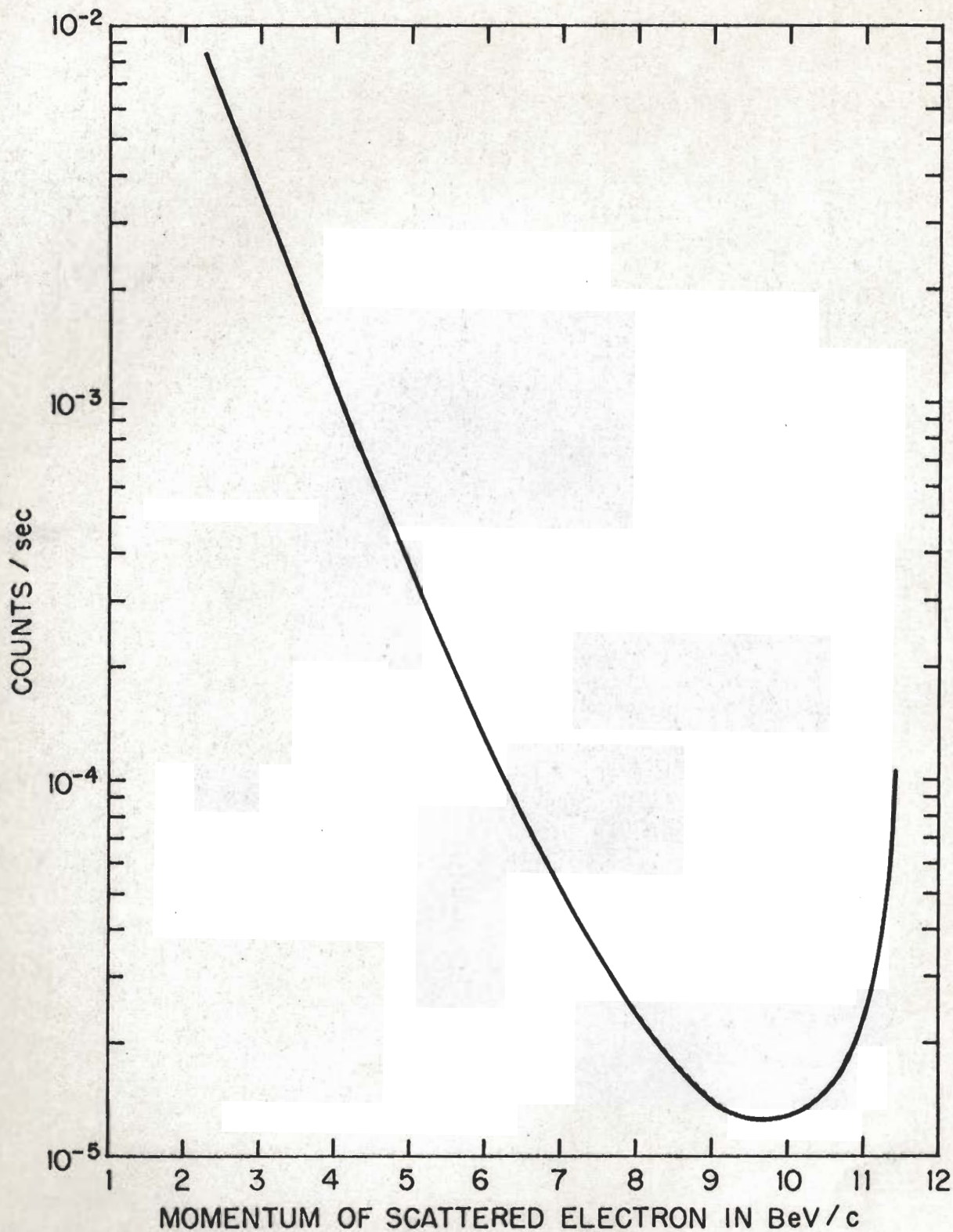
448-13-A

FIG. 11--Radiative tail from elastic peak and (33) resonance.
 The counting rates are obtained with $E_0 = 20$ BeV,
 $\theta = 5^\circ$, 20 cm long liquid hydrogen target, 2×10^{13}
 primary electrons/sec, and 0.1% momentum resolution
 for the 20-BeV/c spectrometer.



448-14-A

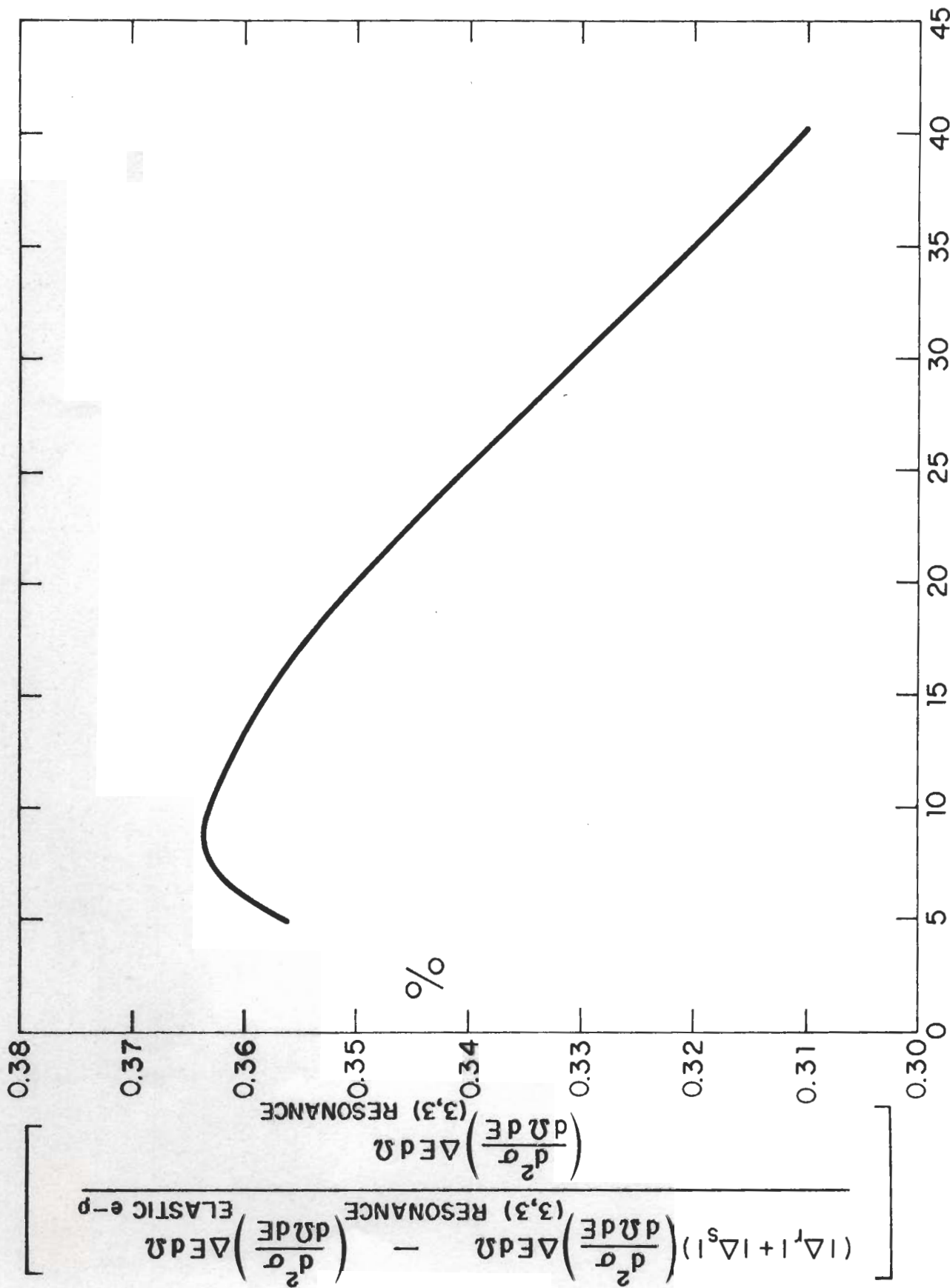
FIG. 12 --Radiative tail from elastic peak and (33) resonance. The counting rates are obtained with $E_0 = 20$ BeV, $\theta = 10^\circ$, 20 cm long liquid hydrogen target, 2×10^{13} primary electrons/sec, and 0.1% momentum resolution for the 20-BeV/c spectrometer.



448-15-A

FIG. 13 --Radiative tail from elastic peak and (33) resonance.

The counting rates are obtained with $E_0 = 20$ BeV,
 $\theta = 15^\circ$, 20 cm long liquid hydrogen target, 2×10^{13}
 primary electrons/sec, and 0.1% momentum resolution
 for the 20-BeV/c spectrometer.



448-46-A

LAB SCATTERING ANGLE θ IN DEGREES

Fig. 14--Radiative correction to 1238 resonance peak height.

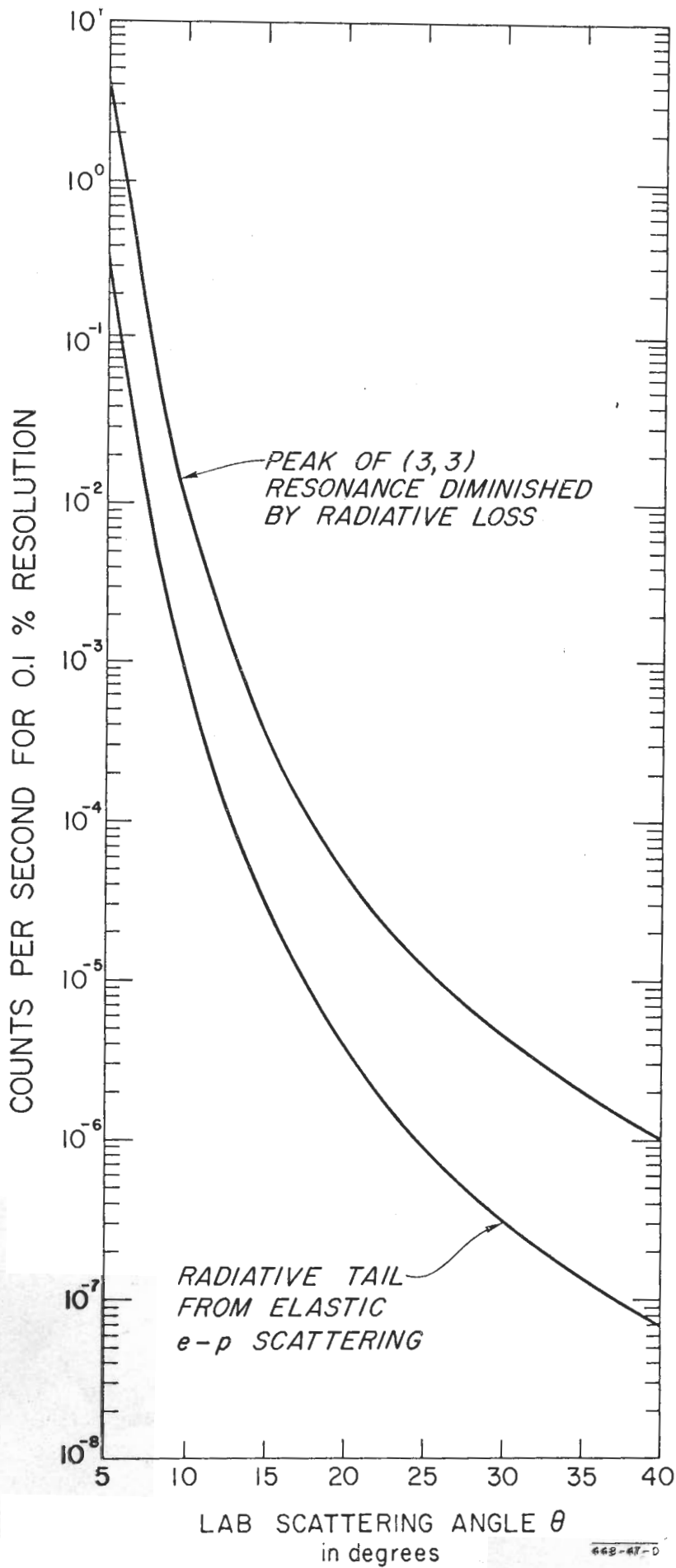


**FIG. 15 - COUNTING RATES FOR PEAK OF (3,3)
 RESONANCE vs SCATTERING ANGLE
 ($E_0 = 20$ BeV)**

REFERENCES

1. W.K.H. Panofsky and E. A. Allton, Phys. Rev. 110, 1155 (1958).
G. G. Ohlsen, Phys. Rev. 120, 584 (1960).
L. N. Hand, Phys. Rev. 129, 1834 (1963).
H. Lynch, J. V. Allaby, D. Ritson, presented at Hamburg Conference, 1965.
2. Cone, et al., Phys. Rev. Letters 14, 326 (1965).
3. S. Fubini, Y. Nambu and V. Wataghin, Phys. Rev. 111, 339 (1958).
4. J. D. Bjorken and J. D. Walecka, SLAC-PUB-139.
5. G. Bellettini, et al., Phys. Letters 18, 167 (1965).